Semi-Supervised Receiver for MIMO Systems with Mixed Khatri-Rao-Kronecker Coding

Amarilton L. Magalhães, Paulo R. B. Gomes, and André L. F. de Almeida

***Abstract*— In this work, we propose a multiple Kronecker product-based space-time (MKronST)-based coding for single-hop point-to-point multiple-input multiple-output (MIMO) systems that employ space-time spreading scheme whose certain number of data streams are spatially spread within the antennas of a subarray while other ones are spread across antennas of different subarrays. Capitalizing on a tensor formalism, the received signals are modelled as a constrained quadrilinear parallel factor (PARAFAC) model, which allows us to derive a semi-supervised iterative receiver for joint symbol and channel estimation. Simulation results are provided to evaluate the performance of the proposed receiver. Our numerical results show that the proposed semi-supervised receiver is capable of jointly estimating the symbol and channel matrices with a superior performance in comparison to competing receivers outlined in the literature.**

***Keywords*— MIMO, constrained PARAFAC model, MKronST coding.**

I. Introduction

In wireless communications, legacy techniques generally deal with signal processing in the matrix form. It is possible employ modern processing techniques that apply tensorial approaches [1] as an effort to exploring dimensions beyond space-time such as frequency, code, azimuth, elevation, polarization, just to mention a few. Getting the most out of all dimensions of the signal can bring advantages such as identifiability, improvement on parameter estimation accuracy, and reliability and robustness on the symbol detection [2]. In multiple-input multiple-output (MIMO) point-to-point communications, the tensorial approach has been used in several works to model different space-time, or space-time-frequency, signaling structures (see [2] and the references therein). Among the existing tensor-based modeling approaches, the most popular makes use of the parallel factor (PARAFAC) decomposition [3], [4], [5], [6]. Following [7], [8], several works have showed the potential of tensor models as powerful tools to model multi-dimensional communication systems while enjoying blind/semi-blind estimation and detection properties [9], [10], [11], [12], [13] and [14]. For instance, in the context of MIMO relaying systems, [10] presented a simplified Khatri-Rao space-time (KRST) coding at the source node and several semi-blind receivers were proposed whose the signals received at the destination node follow a PARATUCK model [15]. The authors of [11] introduced an extra time diversity by using a KRST coding at the relay in a similar transmission scheme in which the signals received at destination were modelled as the nested PARAFAC model originally introduced in [16]. The work [12] proposed a closed-form semi-blind receiver using the Khatri-Rao factorization (KRF) algorithm to achieve a complexity reduction in comparison to previously reported iterative solutions.

More recently, the authors of [17] proposed two new KRST-based coding strategies based on multiple Khatri-Rao and Kronecker products of symbol matrices, called multiple Khatri-Rao product-based space-time (MKRST) and multiple Kronecker product-based space-time (MKronST) codings. Therein, a one-way two-hop MIMO relay system with codings both at the source and relay nodes was considered and semi-blind receivers based on a trilinear PARAFAC-based model were presented. In [18], the authors proposed a two-stage iterative and non-iterative semi-supervised receivers for a MKRST coding based MIMO system, still using a trilinear PARAFAC modeling approach.

In this work we consider a mixed Khatri-Rao-Kronecker based ST coding scheme for point-to-point MIMO system, following up the approach of [17]. In this scheme, the transmit antenna array is partitioned into a certain number of subarrays that transmit Kronecker products of two data streams while spatially spreading these data streams within different antennas of a subarray while other ones are spread across antennas of different subarrays. This approach provides an additional spatial diversity due to the intra-group and inter-group spreadings provided by subarray partitioning. At the destination, we derive a new semi-supervised receiver that exploits a constrained quadrilinear PARAFAC model. In contrast to [17] and [18], which resorts to trilinear PARAFAC models and estimate the transmitted symbols and channels in two stages, our proposed semi-supervised receiver jointly and directly estimates the transmitted symbol and channel matrices by means of a single-stage iterative alternating least squares algorithm. Our numerical results corroborate the performance improvement of the proposed received in terms of symbol error rate over competing solutions, such as the one proposed in [17] while comparing to the its version with perfect channel knowledge.

The rest of this article is organized as follows. In Section II, the notations, preliminaries of tensors and background of PARAFAC decomposition are presented. Section III describes the system model and tensor modelling and in the Section IV, the single stage iterative semi-supervised receiver is derived. On the sequence, in Section V numerical simulations and

Amarilton L. Magalhães and Paulo R. B. Gomes are with the Federal Institute of Education, Science and Technology of Ceará (IFCE), Tauá-CE, Brazil. E-mails: amarilton.magalhaes@ifce.edu.br and paulo.gomes@ifce.edu.br; André L. F. de Almeida is with the Wireless Telecom Research Group (GTEL), Department of Teleinformatics Engineering, Federal University of Ceará, Fortaleza-CE, Brazil. E-mail: andre@gtel.ufc.br.

results are presented for validating the performance of the proposed model, and the article is concluded in Section VI.

II. Notation and Tensor Preliminaries

A. Notation

Scalars, column vectors, matrices, and tensors are denoted by lower-case x, boldface lower-case $\boldsymbol{x}$, boldface capital $\boldsymbol{X}$, and calligraphic $\mathcal{X}$ letters, respectively. $\boldsymbol{X}^{\mathrm{T}}$, $\boldsymbol{X}^{*}$ and $\boldsymbol{X}^{\dagger}$ denote transposition, conjugate and Moore-Penrose pseudo inverse of $\boldsymbol{X}$, respectively. $\boldsymbol{X}_{l:}$ and $\boldsymbol{X}_{:m}$ represent the l-th row and m-th column of $\boldsymbol{X} \in \mathbb{C}^{L\times M}$, respectively. The operator $D_n(\boldsymbol{X})$ forms a diagonal matrix out the n-th row of $\boldsymbol{X}$. A tensor $\mathcal{X} \in \mathbb{C}^{I_1\times I_2\times\cdots\times I_N}$ is a multidimensional data array, in which N is called the order of $\mathcal{X}$. A specific dimension or mode of $\mathcal{X}$ is denoted by I_n, with $n = 1, 2, \ldots, N$. The $(i_1, i_2, \cdots, i_N)$-th entry of $\mathcal{X}$ is denoted by $x_{i_1,i_2,\cdots,i_N}$. Unfolding or matricization is the procedure of reshaping an N-order tensor into a matrix. The mode-n unfolding of $\mathcal{X} \in \mathbb{C}^{I_1\times I_2\times\cdots\times I_N}$ is denoted by $[\mathcal{X}]_{(n)} \in \mathbb{C}^{I_n\times \prod\limits_{m\neq n} I_m}$. For example, given a third-order tensor $\mathcal{X} \in \mathbb{C}^{I\times J\times K}$ with entry $x_{i,j,k}$, the matrices $[\mathcal{X}]_{(1)} \in \mathbb{C}^{I\times JK}$, $[\mathcal{X}]_{(2)} \in \mathbb{C}^{J\times IK}$ and $[\mathcal{X}]_{(3)} \in \mathbb{C}^{K\times IJ}$ denote wide mode-1, mode-2 and mode-3 unfoldings. $||\cdot||_{\mathrm{F}}$ denotes the Frobenious norm and the symbols $\otimes$ and $\diamond$ denote the Kronecker and the Khatri-Rao (columnwise Kronecker) matrix products, respectively. The tensor n-mode product is obtained by multiplying a tensor by a matrix (or a vector) in mode n. Given $\mathcal{X} \in \mathbb{C}^{I_1\times I_2\times\cdots\times I_N}$ and $\boldsymbol{W} \in \mathbb{C}^{J\times I_n}$, their n-mode product is given by $\mathcal{Y} = \mathcal{X} \times_n \boldsymbol{W}$ in a tensor fashion and produces a new tensor $\mathcal{Y} \in \mathbb{C}^{I_1\times\cdots\times I_{n-1}\times J\times I_{n+1}\times\cdots\times I_N}$. It can be computed in the matrix form by $[\mathcal{Y}]_{(n)} = \boldsymbol{W}\,[\mathcal{X}]_{(n)}$.

B. PARAFAC decomposition

The PARAFAC decomposition factorizes a tensor into a sum of R rank-1 tensors. It can be expressed in terms of n-mode products as [1]

$$\mathcal{X} = \mathcal{I}_{N,R} \times_1 \boldsymbol{A}^{(1)} \times_2 \boldsymbol{A}^{(2)} \times \cdots \times_N \boldsymbol{A}^{(N)}, \tag{1}$$

where $\mathcal{I}_{N,R}$ denotes the N-order identity tensor and $\boldsymbol{A}^{(n)} \in \mathbb{C}^{I_n\times R}$ denotes the factor matrices. R is the tensor rank. The elementwise form [3], [6] of the PARAFAC decomposition of a N-th order tensor $\mathcal{X} \in \mathbb{C}^{I_1\times I_2\times\cdots\times I_N}$ is

$$x_{i_1,i_2,\cdots,i_N} = \sum_{r=1}^{R} a^{(1)}_{i_1,r} a^{(2)}_{i_2,r} \cdots a^{(N)}_{i_N,r} = \sum_{r=1}^{R}\prod_{n=1}^{N} a^{(n)}_{i_n,r}, \tag{2}$$

where $a^{(n)}_{i_1r}$ denotes the elements of the factor matrix $\boldsymbol{A}^{(n)}$. The n-mode unfolding of $\mathcal{X}$ admits the following factorization in terms of its factor matrices

$$[\mathcal{X}]_{(n)} = \boldsymbol{A}^{(n)}\left(\boldsymbol{A}^{(N)} \diamond \cdots \diamond \boldsymbol{A}^{(n+1)} \diamond \boldsymbol{A}^{(n-1)} \diamond \cdots \diamond \boldsymbol{A}^{(1)}\right)^{\mathrm{T}}. \tag{3}$$

The most outstanding feature of the PARAFAC decomposition is its essential uniqueness property under mild conditions [1], [15].

III. System Model

Let us consider a point-to-point single user MIMO system with M_s antennas at the source and M_d antennas at the destination. The transmit antenna array is partitioned into K subarrays. We assume a Rayleigh channel model. The signal received $\boldsymbol{X}$ at the destination can be expressed as

$$\boldsymbol{X} = \boldsymbol{H}\boldsymbol{S}^{\mathrm{T}} + \boldsymbol{V}, \tag{4}$$

where $\boldsymbol{H} \in \mathbb{C}^{M_d\times M_s}$ is the channel matrix, $\boldsymbol{V}$ is the additive white Gaussian noise (AWGN) term, and $\boldsymbol{S}$ denotes the coded symbol matrix. The transmission rate, expressed by bits per channel use, is given by $\rho = \frac{n_{us}}{n_{ps}}\log_2\nu$, where n_{us} is the number of information symbols contained in $\boldsymbol{S}$, n_{ps} is the number of symbol periods, and ν denotes the modulation cardinality (constellation size).

We consider a space-time spreading scheme such that M_s/K data streams spanning N_1 symbol periods are spatially spread within the antennas of a subarray (intra-group spreading), while K data streams spanning N_2 symbol periods are spread across the antennas of different subarrays (inter-group spreading). The data transmission embeds M_s pilot sequences spanning N_p symbols. We consider that the first information symbol in each data stream is known at the receiver. The overall transmitted symbol matrix is generated according to a MKronST-based coding, in which $\boldsymbol{S}$ is formed through the Khatri-Rao product of a pilot matrix $\boldsymbol{S}_p \in \mathbb{C}^{N_p\times M_s}$ and a Kronecker product of various symbol matrices $\boldsymbol{S}^{(q)} \in \mathbb{C}^{N_q\times M_{s_q}}$, with $q = 1, 2, \cdots, Q$, and $Q \geq 2$, as follows

$$\begin{aligned}\boldsymbol{S} &= \boldsymbol{S}_p \diamond \left[\boldsymbol{S}^{(1)} \otimes \boldsymbol{S}^{(2)} \otimes \cdots \otimes \boldsymbol{S}^{(Q)}\right] \\ &= \boldsymbol{S}_p \diamond \bigotimes_{q=1}^{Q} \boldsymbol{S}^{(q)}.\end{aligned} \tag{5}$$

For simplicity of exposition, we consider $N = 2$ and propose to rewrite (5) as

$$\boldsymbol{S} = \boldsymbol{S}_p \diamond \boldsymbol{S}_2\boldsymbol{\Phi} \diamond \boldsymbol{S}_1\boldsymbol{\Psi}, \tag{6}$$

where $\boldsymbol{S}_p \in \mathbb{C}^{N_pN_2N_1\times M_s}$ denotes the pilot matrix, $\boldsymbol{S}_1 \in \mathbb{C}^{N_1\times M_s/K}$ and $\boldsymbol{S}_2 \in \mathbb{C}^{N_2\times K}$ are the two symbol matrices carrying the information symbols, while $\boldsymbol{\Psi} \in \mathbb{C}^{M_s/K\times M_s}$ and $\boldsymbol{\Phi} \in \mathbb{C}^{K\times M_s}$ are constraint matrices defined as $\boldsymbol{\Psi} = \boldsymbol{1}^{\mathrm{T}}_K \otimes \boldsymbol{I}_{\frac{M_s}{K}}$ and $\boldsymbol{\Phi} = \boldsymbol{I}_K \otimes \boldsymbol{1}^{\mathrm{T}}_{\frac{M_s}{K}}$, respectively. These constraint matrices satisfy the Khatri-Rao structure $\boldsymbol{\Phi} \diamond \boldsymbol{\Psi} = \boldsymbol{I}_{M_s}$. The product $\boldsymbol{S}_1\boldsymbol{\Psi}$ concatenates K matrices $\boldsymbol{S}_1$ side by side, while the product $\boldsymbol{S}_2\boldsymbol{\Phi}$ produces a matrix in which each column of $\boldsymbol{S}_2$ is repeated M_s/K times. The constraint matrices $\boldsymbol{\Psi}$ and $\boldsymbol{\Phi}$ have a physical interpretation. Indeed, they capture the intragroup and intergroup spreading structures, respectively. For instance, when $M_s = 4$ and $K = 2$, we have

$$\boldsymbol{\Psi} = \begin{bmatrix}1 & 0 & 1 & 0\\ 0 & 1 & 0 & 1\end{bmatrix},\ \boldsymbol{\Phi} = \begin{bmatrix}1 & 1 & 0 & 0\\ 0 & 0 & 1 & 1\end{bmatrix}. \tag{7}$$

From the property $\boldsymbol{S}_2\boldsymbol{\Phi} \diamond \boldsymbol{S}_1\boldsymbol{\Psi} = (\boldsymbol{S}_2 \otimes \boldsymbol{S}_1)(\boldsymbol{\Phi} \diamond \boldsymbol{\Psi})$, we have $\boldsymbol{S}_2\boldsymbol{\Phi} \diamond \boldsymbol{S}_1\boldsymbol{\Psi} = \boldsymbol{S}_2 \otimes \boldsymbol{S}_1$ since the Khatri-Rao product between $\boldsymbol{\Phi}$ and $\boldsymbol{\Psi}$ is equal to identity matrix.

By substituting (6) into (4), we can recast the received signal matrix $\boldsymbol{X} \in \mathbb{C}^{M_d\times N_pN_2N_1}$ as a fourth-order tensor

$\mathcal{X} \in \mathbb{C}^{M_d \times N_1 \times N_2 \times N_p}$ that can be expressed using the n-mode product notation as

$$\mathcal{X} = \mathcal{I}_{4,M_s} \times_1 \boldsymbol{H} \times_2 \boldsymbol{S}_1\boldsymbol{\Psi} \times_3 \boldsymbol{S}_2\boldsymbol{\Phi} \times_4 \boldsymbol{S}_p + \mathcal{V}, \quad (8)$$

where $\mathcal{I}_{4,M_s}$ represents a fourth-order identity tensor of size $M_s \times M_s \times M_s \times M_s$, and $\mathcal{V}$ is the corresponding noise tensor. The signal part of (8) follows a constrained quadrilinear PARAFAC model with factor matrices represented by $\boldsymbol{H}$, $\boldsymbol{S}_1\boldsymbol{\Psi}$, $\boldsymbol{S}_2\boldsymbol{\Phi}$ and $\boldsymbol{S}_p$. The tensor $\mathcal{X}$ admits the following factorizations with respect to their factor matrices:

$$[\mathcal{X}]_{(1)} = \boldsymbol{H}\left(\boldsymbol{S}_p \diamond (\boldsymbol{S}_2\boldsymbol{\Phi}) \diamond (\boldsymbol{S}_1\boldsymbol{\Psi})\right)^{\mathrm{T}} + [\mathcal{V}]_{(1)}, \quad (9)$$

$$[\mathcal{X}]_{(2)} = \boldsymbol{S}_1\boldsymbol{\Psi}\left(\boldsymbol{S}_p \diamond (\boldsymbol{S}_2\boldsymbol{\Phi}) \diamond \boldsymbol{H}\right)^{\mathrm{T}} + [\mathcal{V}]_{(2)}, \quad (10)$$

$$[\mathcal{X}]_{(3)} = \boldsymbol{S}_2\boldsymbol{\Phi}\left(\boldsymbol{S}_p \diamond (\boldsymbol{S}_1\boldsymbol{\Psi}) \diamond \boldsymbol{H}\right)^{\mathrm{T}} + [\mathcal{V}]_{(3)}, \quad (11)$$

$$[\mathcal{X}]_{(4)} = \boldsymbol{S}_p\left((\boldsymbol{S}_2\boldsymbol{\Phi}) \diamond (\boldsymbol{S}_1\boldsymbol{\Psi}) \diamond \boldsymbol{H}\right)^{\mathrm{T}} + [\mathcal{V}]_{(4)}. \quad (12)$$

IV. Proposed Receiver

In this section, we present an iterative semi-supervised receiver for joint channel and symbol estimation that exploits the quadrilinear PARAFAC tensor model derived in the previous section. The receiver makes use of the three unfoldings of the received signal tensor given in (9)-(11) to jointly estimate the channel matrix $\boldsymbol{H}$ and the symbol matrices $\boldsymbol{S}_1$ and $\boldsymbol{S}_2$ by means of a trilinear alternating least-squares (ALS) algorithm. The algorithm alternately estimate each matrix by solving the following conditional LS criteria:

$$\underset{\boldsymbol{H}}{\operatorname{argmin}} \left|\left|[\mathcal{X}]_{(1)} - \boldsymbol{H}\left(\boldsymbol{S}_p \diamond (\boldsymbol{S}_2\boldsymbol{\Phi}) \diamond (\boldsymbol{S}_1\boldsymbol{\Psi})\right)^{\mathrm{T}}\right|\right|_{\mathrm{F}}^2, \quad (13)$$

$$\underset{\boldsymbol{S}_1}{\operatorname{argmin}} \left|\left|[\mathcal{X}]_{(2)} - \boldsymbol{S}_1\boldsymbol{\Psi}\left(\boldsymbol{S}_p \diamond (\boldsymbol{S}_2\boldsymbol{\Phi}) \diamond \boldsymbol{H}\right)^{\mathrm{T}}\right|\right|_{\mathrm{F}}^2, \quad (14)$$

$$\underset{\boldsymbol{S}_2}{\operatorname{argmin}} \left|\left|[\mathcal{X}]_{(3)} - \boldsymbol{S}_2\boldsymbol{\Phi}\left(\boldsymbol{S}_p \diamond (\boldsymbol{S}_1\boldsymbol{\Psi}) \diamond \boldsymbol{H}\right)^{\mathrm{T}}\right|\right|_{\mathrm{F}}^2, \quad (15)$$

the solutions of which are given, respectively, by

$$\hat{\boldsymbol{H}} = [\mathcal{X}]_{(1)}\left[\left(\boldsymbol{S}_p \diamond (\boldsymbol{S}_2\boldsymbol{\Phi}) \diamond (\boldsymbol{S}_1\boldsymbol{\Psi})\right)^{\mathrm{T}}\right]^{\dagger}, \quad (16)$$

$$\hat{\boldsymbol{S}}_1 = [\mathcal{X}]_{(2)}\left[\boldsymbol{\Psi}\left(\boldsymbol{S}_p \diamond (\boldsymbol{S}_2\boldsymbol{\Phi}) \diamond \boldsymbol{H}\right)^{\mathrm{T}}\right]^{\dagger}, \quad (17)$$

$$\hat{\boldsymbol{S}}_2 = [\mathcal{X}]_{(3)}\left[\boldsymbol{\Phi}\left(\boldsymbol{S}_p \diamond (\boldsymbol{S}_1\boldsymbol{\Psi}) \diamond \boldsymbol{H}\right)^{\mathrm{T}}\right]^{\dagger}, \quad (18)$$

where $\hat{\boldsymbol{H}}$, $\hat{\boldsymbol{S}}_1$ and $\hat{\boldsymbol{S}}_2$ denote the estimates of $\boldsymbol{H}$, $\boldsymbol{S}_1$ and $\boldsymbol{S}_2$, respectively. At the receiver, each iteration of the trilinear ALS algorithm contains three updating steps. At each step, the fitting error is minimized with respect to one given factor matrix by fixing the others to their values obtained at previous updating steps. This procedure is repeated until convergence is reached. The error at the i-th iteration is calculated as

$$e_{(i)} = \left|\left|[\mathcal{X}]_{(1)} - \hat{\boldsymbol{H}}_{(i)}\left[\boldsymbol{S}_p \diamond (\hat{\boldsymbol{S}}_{2_{(i)}}\boldsymbol{\Phi}) \diamond (\hat{\boldsymbol{S}}_{1_{(i)}}\boldsymbol{\Psi})\right]^{\mathrm{T}}\right|\right|_{\mathrm{F}}^2,$$

and the convergence is declared when $\left|e_{(i)} - e_{(i-1)}\right| / e_{(i)} < \varepsilon$. In Algorithm 1, the proposed receiver for direct symbol and channel estimation is summarized, herein refereed to as the constrained trilinear ALS (CTALS) receiver.

Algorithm 1: Proposed constrained trilinear ALS (CTALS) for direct joint symbol and channel estimation.

1. *Set* $i = 0$; *Initialize* $\hat{\boldsymbol{S}}_{1(i=0)}$ and $\hat{\boldsymbol{S}}_{2(i=0)}$ *randomly*;
2. $i = i + 1$;
3. *Using* $[\mathcal{X}]_{(1)}$, *find an LS estimate of* $\hat{\boldsymbol{H}}_{(i)}$:
$$\hat{\boldsymbol{H}}_{(i)} = [\mathcal{X}]_{(1)}\left[\left(\hat{\boldsymbol{S}}_p \diamond \left[\hat{\boldsymbol{S}}_{2(i-1)} \otimes \hat{\boldsymbol{S}}_{1(i-1)}\right]\right)^{\mathrm{T}}\right]^{\dagger};$$
4. *Using* $[\mathcal{X}]_{(2)}$, *find an LS estimate of* $\hat{\boldsymbol{S}}_{1(i)}$:
$$\hat{\boldsymbol{S}}_{1(i)} = [\mathcal{X}]_{(2)}\left[\boldsymbol{\Psi}\left(\hat{\boldsymbol{S}}_p \diamond \hat{\boldsymbol{S}}_{2(i-1)}\boldsymbol{\Phi} \diamond \hat{\boldsymbol{H}}_{(i)}\right)^{\mathrm{T}}\right]^{\dagger};$$
5. *Using* $[\mathcal{X}]_{(3)}$, *find an LS estimate of* $\hat{\boldsymbol{S}}_{2(i)}$:
$$\hat{\boldsymbol{S}}_{2(i)} = [\mathcal{X}]_{(3)}\left[\boldsymbol{\Phi}\left(\hat{\boldsymbol{S}}_p \diamond \hat{\boldsymbol{S}}_{1(i)}\boldsymbol{\Psi} \diamond \hat{\boldsymbol{H}}_{(i)}\right)^{\mathrm{T}}\right]^{\dagger};$$
6. *Repeat steps 2-5 until convergence*;
7. *Remove scaling ambiguities*;
8. *Project the estimated symbols onto the alphabet.*

Since the pilot matrix $\boldsymbol{S}_p$ is known at the receiver, permutation ambiguity does not exist However, the estimates of the symbol and channel matrices $\hat{\boldsymbol{S}}_1$, $\hat{\boldsymbol{S}}_2$ and $\hat{\boldsymbol{H}}$ are affected by scaling ambiguities. To remove the scaling factors of $\boldsymbol{S}_1$ and $\boldsymbol{S}_2$, we consider that the first row of these matrices is known and composed of 1's. This corresponds to using ID bits that are fixed by the transmitted and known at the receiver for each transmission. Hence, these known symbols are then used to find the final estimates of the symbol matrices as follows

$$\bar{\hat{\boldsymbol{S}}}_1 = \hat{\boldsymbol{S}}_1\boldsymbol{\Delta}_{\boldsymbol{S}_1}, \quad \bar{\hat{\boldsymbol{S}}}_2 = \hat{\boldsymbol{S}}_2\boldsymbol{\Delta}_{\boldsymbol{S}_2},$$

where $\boldsymbol{\Delta}_{\boldsymbol{S}_1} = [D_1(\boldsymbol{S}_1)]^{-1}$ and $\boldsymbol{\Delta}_{\boldsymbol{S}_2} = [D_1(\boldsymbol{S}_2)]^{-1}$. Since the scaling ambiguities compensate each other, the matrix that corrects the scaling ambiguity on the estimated channel matrix is given by $\boldsymbol{\Delta}_{\boldsymbol{H}} = D_1\left(\overline{\boldsymbol{S}}_2\right) D_1\left(\overline{\boldsymbol{S}}_1\right)$, from which a final estimate of the channel matrix can be obtained as $\bar{\hat{\boldsymbol{H}}} = \hat{\boldsymbol{H}}\boldsymbol{\Delta}_{\boldsymbol{H}}$.

V. Simulation results and discussion

The performance of the proposed CTALS receiver is evaluated in terms of symbol error rate (SER) and normalized mean square error (NMSE) of the estimated channel, as a function of the signal-to-noise ratio (SNR). Each SER and NMSE curve is an average of 1000 independent Monte Carlo runs. Each run corresponds to a different realization of channel, symbol, and noise matrices. For each run, the NMSE is calculated as $\left|\left|\boldsymbol{H} - \hat{\boldsymbol{H}}\right|\right|_{\mathrm{F}}^2 / ||\boldsymbol{H}||_{\mathrm{F}}^2$. The coefficients of the MIMO channel matrix are drawn from a zero-mean unit-variance complex-valued Gaussian distribution (Rayleigh fading assumption), while the symbol matrices $\boldsymbol{S}_1$ and $\boldsymbol{S}_2$ are drawn from a 16-QAM (quadrature amplitude modulation) constellation. The pilot symbol matrix $\boldsymbol{S}_p$ is designed as a truncated discrete Fourier transform (DFT) matrix. The noise power is generated according to the desired SNR. Since we assume that the first row of each symbol matrix is fixed, the effective transmission rate of the mixed Khatri-Rao-Kronecker can be calcutated with $n_{us} = (N_1 - 1)\frac{M_s}{K} + (N_2 - 1)K$, $n_{ps} = N_p N_1 N_2$, and $\nu = 16$.

In Figures 1 and 2, we compare SER and NMSE performances of the proposed receiver CTALS with: (i) the traditional trilinear ALS (TALS) [16] and multidimensional Khatri-Rao factorization [19] of three matrices (KRF3) methods for systems that employ MKRST coding [17], [18]; (ii) the two-stage KRF-KronF receiver [17]; (iii) the single-stage BALS (bilinear ALS) assuming a perfect knowlegde of the MIMO channel matrix to estimate the individual symbol matrices. More specifically, this receiver is a bilinear version of what is designed from Algorithm 1. Note that the two-stage receivers TALS, KRF3, and KRF-KronF also exploit the MKronST coding scheme given by (5), but are instead based on a trilinear PARAFAC model [17]. To ensure a fair comparison with the TALS and KRF3 receivers that are valid for the MKRST coding scheme [17], the transmission parameters of the MKronST scheme are adjusted to ensure the same the transmission rate as that of the MKRST scheme[1]. To this end, we set $M_s = M_d = N_1 = N_2 = 4$, and use $N_p = 6$ for MKronST and $N_p = 12$ for MKRST.

From Figure 1, we can note that the CTALS receiver outperforms all the competing receivers. Although both TALS and CTALS exploit a quadrilinear PARAFAC model, the performance gains of CTALS comes from the improved symbol estimation accuracy achieved with the intergroup/intragroup spatial spreading that introduces an extra spatial diversity, whereas TALS is based on the conventional PARAFAC model with Khatri-Rao coding which is a full spatial multiplexing scheme. As for the channel estimation, we can see that TALS, KRF3 and CTALS have the same NMSE performance. Note also that the KRF-KronF receiver has the worst performance due to the error propagation that affects the symbol estimation in the second stage. It is worth noting that the SER performance of CTALS is slightly inferior to that of the BALS with perfect channel knowledge.

In Figure 2, the NMSE results of estimated channel are shown. We can see that CTALS has the same channel estimation accuracy as the TALS and KRF3 receivers, which is in turn better than that of the KRF-KronF receiver. Indeed, CTALS and TALS are iterative estimation algorithms that provide a direct and joint estimation of the symbol and channel matrices, while KRF3 jointly estimates the symbol and channel matrices in closed form.

In Figure 3, we compare SER performances for KRF-KronF and CTALS receivers, in which the number of symbol periods is varied as $N_1 = N_2 = 2$, 4 and 8. The number of transmitting antennas, receiving antennas and pilot symbols are fixed to $M_s = M_d = N_p = 4$, respectively, and the number of subarrays is set to $K = 2$. When we analyse the influence of the data block lengths $N_1 = N_2$, we conclude that a slight improvement in the SER is achieved when N_1/N_2 increases. Since the transmission rate is reduced when N_1 or N_2 increases, using short data blocks is recommended.

In Figure 4, we consider the proposed CTALS receiver and evaluate the individual SER performance of the symbol matrices $\boldsymbol{S}_1$ and $\boldsymbol{S}_2$ for two system configurations with $N_1 = 10$, $N_2 = 2$ and $N_1 = 2$, $N_2 = 10$. We can observe that the SER of $\boldsymbol{S}_1$ is better than that of $\boldsymbol{S}_2$ in the second configuration

[1]The transmission rate for the MKRST coding scheme can be calculated with $n_{us} = [(N_1 - 1) + (N_2 - 1)]M_s$ and $n_{ps} = N_p N_2 N_1$ [17].

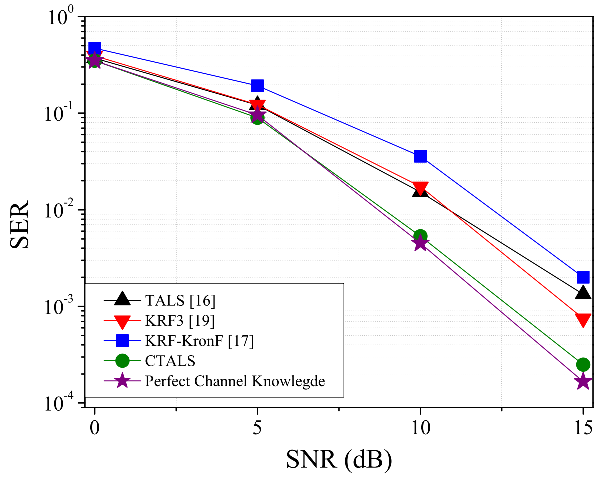

Fig. 1. SER vs. SNR comparison for various receivers.

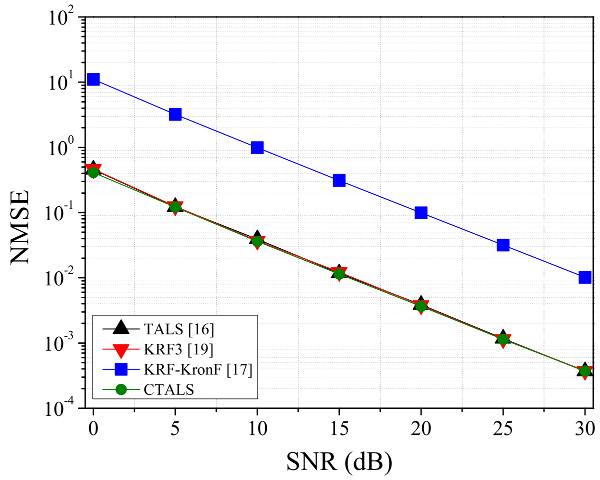

Fig. 2. NMSE of estimated channel vs. SNR comparison for various receivers.

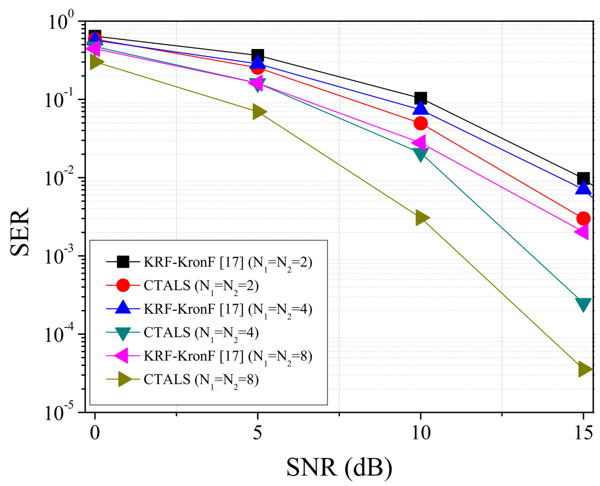

Fig. 3. SER vs. SNR comparison for $N_1 = N_2 = 2$, 4 and 8.

($N_1 = 2$ and $N_2 = 10$). Conversely, the SER of $\boldsymbol{S}_2$ is better than that of $\boldsymbol{S}_1$ in the first configuration ($N_1 = 10$ and $N_2 = 2$). This results corroborate the cross-spreading gains

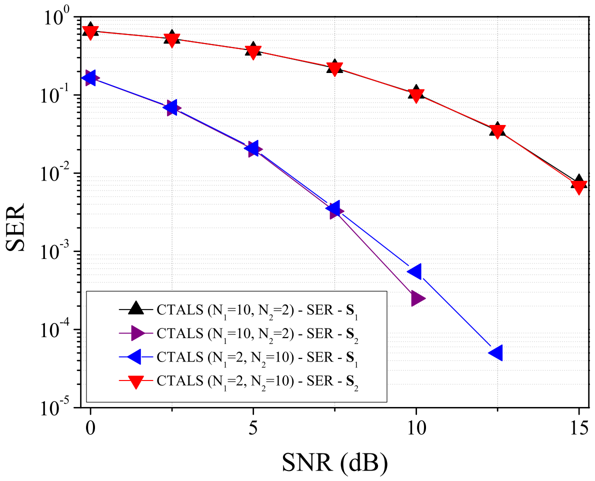

Fig. 4. SER vs. SNR comparison for the CTALS receiver under two scenarios with the block length configurations ($N_1 = 2$, $N_2 = 10$) and ($N_1 = 10$, $N_2 = 2$).

of the MKronST scheme, where $\boldsymbol{S}_1$ acts as a spreading code for $\boldsymbol{S}_2$ and vice-versa. Thus, increasing the time span of one matrix leads to a performance improvement on the detection of the other matrix. A similar behavior was observed in the KRF-KRF receiver of [18].

VI. Conclusions

We have proposed an iterative semi-supervised CTALS receiver for MKronST-coded MIMO systems. The proposed receiver jointly and directly estimates the transmitted symbol and channel matrices by means of a single-stage iterative alternating least squares algorithm that capitalizes on a constrained quadrilinear PARAFAC model for the received signal tensor. Our numerical results corroborate the performance improvement of the proposed receiver in comparison to competing alternatives, in terms of symbol error rate and channel normalized mean square error. As future perspectives of this work, we shall consider the generalization of the presented model to the multi-user case and extended spreading schemes that can incorporate an extra frequency (or time) dimension by operating with pilot symbol tensors (instead of pilot symbol matrices). The development of new receiver algorithms to deal with such schemes is also a topic for future studies.

Acknowlegments

The authors are thankful to Coordenação de Aperfeiçoamento de Pessoal de Nível Superior CAPES - Brasil for partially supporting this work (Finance Code 001). The research of André L. F. de Almeida is partially supported by CNPq.

References

[1] T. G. Kolda and B. W. Bader, “Tensor decompositions and applications,” *SIAM review*, vol. 51, no. 3, pp. 455–500, 2009.

[2] A. L. F. de Almeida, G. Favier, J. da Costa, and J. C. M. Mota, “Overview of tensor decompositions with applications to communications,” in *Signals and Images: Advances and Results in Speech, Estimation, Compression, Recognition, Filtering, and Processing*. CRC Press, 2016, pp. 325–356.

[3] F. L. Hitchcock, “The expression of a tensor or a polyadic as a sum of products,” *Journal of Mathematics and Physics*, vol. 6, no. 1-4, pp. 164–189, 1927.

[4] A. Cichocki, D. Mandic, L. De Lathauwer, G. Zhou, Q. Zhao, C. Caiafa, and H. A. Phan, “Tensor decompositions for signal processing applications: From two-way to multiway component analysis,” *IEEE signal processing magazine*, vol. 32, no. 2, pp. 145–163, 2015.

[5] R. A. Harshman *et al.*, “Foundations of the PARAFAC procedure: Models and conditions for an" explanatory" multimodal factor analysis,” *UCLA Working Pap. Phonet*, vol. 16, pp. 1–84, 1970.

[6] J. D. Carroll and J.-J. Chang, “Analysis of individual differences in multidimensional scaling via an N-way generalization of “Eckart-Young” decomposition,” *Psychometrika*, vol. 35, no. 3, pp. 283–319, 1970.

[7] N. D. Sidiropoulos, G. B. Giannakis, and R. Bro, “Blind PARAFAC receivers for DS-CDMA systems,” *IEEE Transactions on Signal Processing*, vol. 48, no. 3, pp. 810–823, 2000.

[8] N. D. Sidiropoulos and R. S. Budampati, “Khatri-Rao space-time codes,” *IEEE Transactions on Signal Processing*, vol. 50, no. 10, pp. 2396–2407, 2002.

[9] K. Liu, J. P. C. Da Costa, H.-C. So, and A. L. De Almeida, “Semi-blind receivers for joint symbol and channel estimation in space-time-frequency MIMO-OFDM systems,” *IEEE Transactions on Signal Processing*, vol. 61, no. 21, pp. 5444–5457, 2013.

[10] L. R. Ximenes, G. Favier, A. L. de Almeida, and Y. C. Silva, “PARAFAC-PARATUCK semi-blind receivers for two-hop cooperative MIMO relay systems,” *IEEE Transactions on Signal Processing*, vol. 62, no. 14, pp. 3604–3615, 2014.

[11] L. R. Ximenes, G. Favier, and A. L. de Almeida, “Semi-blind receivers for non-regenerative cooperative MIMO communications based on nested PARAFAC modeling,” *IEEE Transactions on Signal Processing*, vol. 63, no. 18, pp. 4985–4998, 2015.

[12] ——, “Closed-form semi-blind receiver for MIMO relay systems using double Khatri–Rao space-time coding,” *IEEE Signal Processing Letters*, vol. 23, no. 3, pp. 316–320, 2016.

[13] D. S. Rocha, G. Favier, and C. A. R. Fernandes, “Closed-form receiver for multi-hop MIMO relay systems with tensor space-time coding,” *Journal of Communication and Information Systems*, vol. 34, no. 1, pp. 50–54, 2019.

[14] R. K. Miranda, J. P. C. da Costa, B. Guo, A. L. de Almeida, G. Del Galdo, and R. T. de Sousa, “Low-complexity and high-accuracy semi-blind joint channel and symbol estimation for massive MIMO-OFDM,” *Circuits, Systems, and Signal Processing*, vol. 38, no. 3, pp. 1114–1136, 2019.

[15] R. A. Harshman and M. E. Lundy, “Uniqueness proof for a family of models sharing features of Tucker’s three-mode factor analysis and PARAFAC/CANDECOMP,” *Psychometrika*, vol. 61, no. 1, pp. 133–154, 1996.

[16] A. L. de Almeida and G. Favier, “Double Khatri–Rao space-time-frequency coding using semi-blind PARAFAC based receiver,” *IEEE Signal Processing Letters*, vol. 20, no. 5, pp. 471–474, 2013.

[17] W. Freitas Jr, G. Favier, and A. L. de Almeida, “Generalized Khatri-Rao and Kronecker space-time coding for MIMO relay systems with closed-form semi-blind receivers,” *Signal Processing*, vol. 151, pp. 19–31, 2018.

[18] P. H. de Pinho, C. M. FKB, G. Favier, C. da Costa João Paulo, L. de Almeida André, and J. Maranhão, “Semi-supervised receivers for MIMO systems with multiple Khatri-Rao coding,” in *2019 13th International Conference on Signal Processing and Communication Systems (ICSPCS)*. IEEE, 2019, pp. 1–7.

[19] M. Weis, F. Roemer, M. Haardt, and P. Husar, “Dual-symmetric parallel factor analysis using Procrustes estimation and Khatri-Rao factorization,” in *2012 Proceedings of the 20th European Signal Processing Conference (EUSIPCO)*. IEEE, 2012, pp. 270–274.